Clim Dyn
DOI 10.1007/s00382-012-1601-z

Polar amplification: is atmospheric heat transport important?

Vladimir A. Alexeev · Craig H. Jackson

Received: 4 April 2012 / Accepted: 12 November 2012

Abstract Surface albedo feedback is widely believed to be the principle contributor to polar amplification. However, a number of studies have shown that coupled ocean-atmosphere models without ice albedo feedbacks still produce significant polar amplification in 2 × CO_2 runs due to atmospheric heat transports and their interaction with surface conditions. In this article, the relative importance of atmospheric heat transport and surface albedo is assessed using a conceptual 2-box energy balance model in a variety of different model climates. While both processes are shown to independently contribute to the polar amplified response of the model, formal feedback analysis indicates that a strong surface albedo response will tend to reduce the effect of atmospheric heat transport in the full model. We identify several scenarios near the present day climate in which, according to this formal feedback analysis, atmospheric heat transport plays no role in shaping the equilibrium warming response to uniform forcing. However, a closer analysis shows that even in these scenarios the presence of atmospheric heat transport feedback does play a significant role in shaping the trajectory by which the climate adjusts to its new equilibrium.

V. A. Alexeev (✉)
International Arctic Research Center,
University of Alaska, Fairbanks,
930 Koyukuk Drive, Fairbanks, AK 99775, USA
e-mail: valexeev@iarc.uaf.edu

C. H. Jackson
Ohio Wesleyan University,
90 S Henry St,
Delaware, OH 43015, USA
e-mail: chjackso@owu.edu

Keywords Global warming · Polar amplification · Albedo feedback · Atmospheric heat transport

1 Introduction

In 1896, S. Arrhenius proposed the possibility of global warming as a result of increases in the concentration of greenhouse gases. He came to this conclusion based on earlier work done by other scientists (Langley, Tyndall, Lecher, Pernter, Paschen, Aangstroem and others). His calculations included effects of water vapor on radiative absorption in the atmosphere and changes in surface albedo because of snow. He arrived at a global mean temperature increase of about 5 °C as a result of doubling the CO_2 concentration. Remarkably, these results exhibited the polar amplified shape of global warming, with greater effects in the winter. The calculations were done 'locally' at specific latitudes based on observations of radiative fluxes under different atmospheric conditions (air temperature and moisture). This approach, taking into account the dependence of available moisture on the atmospheric air temperature, is a good zero-order model of the greenhouse effect in our climate system, although Arrhenius did not consider many other important components (e.g., clouds). Arrhenius later revised his 2 × CO_2 estimates of temperature change downwards based on different assumptions of the effect of water vapor.

Many years have passed since those first very simple calculations, but the original Arrhenius estimate of what today is called the global warming response to doubling the CO_2 concentration still holds as it is well within the range of potential estimates as determined by a suite of IPCC models (IPCC 2007).

Published online: 05 December 2012

1.1 Surface albedo feedback as a major polar amplification mechanism

Polar amplification (PA) is the phenomenon by which a global warming (or cooling) of the Earth tends to be amplified at the poles. Polar amplification can be easily understood as a result of disappearance of snow/sea ice, which is often called the positive surface albedo feedback (SAF): the more snow/ice, the more sunlight gets reflected back thus creating the potential for colder temperatures which forms even more snow and/or sea ice and a greater area of high albedo surface.

Energy balance models (EBM) have been widely used to gain insight into the relative roles of individual climate processes and to obtain simple estimates of future climates. Their use continues even in the era of fully coupled GCMs due to their low computational overhead and their ability to focus attention on the particular climate process one wishes to study. An energy balance model is usually based on simple expressions for top-of-atmosphere (TOA) radiation and heat transport in the atmosphere given in terms of the surface temperature. The atmosphere is assumed to be in balance with the TOA and the surface budgets. Fluxes at the surface, therefore, can be calculated as a residual in order to close the energy balance of the system. A simple ocean (e.g. slab ocean) of some kind responds to the surface fluxes and the atmosphere is often assumed to have negligible heat capacity.

The early to mid-1960s were marked by groundbreaking results by Budyko (1969) and Sellers (1969) on modeling changes in the global temperature using energy balance models. These models were used to explain possible ice ages and to predict ranges of future temperature change. Both models incorporated ice albedo feedback and therefore resulted in PA. The theory of energy balance models has been developed further by North (1975), Robock (1983), and other authors.

A central concern of energy balance models is parametrization of TOA radiation. Various estimates have been obtained for coefficients in the Budyko-Sellers parameterization of TOA radiation (Stone 1973, North 1975). The remarkable thing about these estimates is the constancy of the linear parameter, B, responsible for sensitivity of outgoing longwave radiation (OLR) to surface temperature, obtained from different sources and models. One important thing often overlooked in using this parameterization is that it includes, in some form, the effect of increase in moisture content with increasing temperature due to the Clausius-Clapeyron dependency (Lindberg 2003).

Langen and Alexeev (2005a, b) verified the applicability of the Budyko-Sellers type of TOA radiative parameterization under uniform forcing using two different GCMs. They also found that if anything, the coefficient B responsible for the outgoing TOA radiation in the tropical zone could only be smaller than the corresponding coefficient for the extra-tropical zone. This would imply a seemingly unexpected equatorially amplified response to a uniformly applied forcing if sensitivity of the atmospheric heat transport were not taken into account. The importance of accurate representations of coupling between components of the climate system engine is, therefore, of prime importance. Proper representation of interaction between the TOA and surface budgets with atmospheric poleward transports was stressed in Alexeev and Bates (1999).

SAF makes the climate system strongly nonlinear. It can be easily understood in terms of step-function-like behavior of surface albedo and therefore reflected solar radiation as a function of temperature. Multiple equilibria can be obtained in energy balance models with surface albedo feedbacks. Manabe and Stouffer (1988) wrote a groundbreaking article showing the possibility of multiple equilibrium states in a GCM under similar external forcing conditions. This idea was further developed in Rahmstorf (1995). Studies with more complex models (EMICs and GCMs) show similar results as e.g. in Langen and Alexeev (2004).

1.2 PA in systems without surface albedo feedbacks

Although surface albedo feedbacks have been recognized as prominently contributing to higher sensitivity of high-latitude climates (e.g. Holland and Bitz 2003), other mechanisms may also be contributing significantly to observed and modeled polar amplification.

It was probably Flannery (1984) who first demonstrated the importance of atmospheric heat transport (AHT) for PA in a model without surface albedo feedbacks. He analyzed a simple energy balance model capable of transporting 'both thermal energy of air and latent heat associated with water vapor.' He also coined the term 'polar amplification.' Inclusion of the latent heat transport component allowed Flannery to explain polar amplification 'in terms of a temperature dependent effective diffusion coefficient that increases with warming.'

Significant PA in a model without any sea ice or other surface albedo feedbacks was obtained in a number of studies with models of different complexity (Flannery 1984; Schneider et al. 1997; Alexeev 2003 [A03]; Rodgers et al. 2003; Alexeev et al. 2005 [ALB05]; Langen and Alexeev 2005a, b; Cai 2005; Langen and Alexeev 2007 [LA07]; Graversen and Wang 2009).

A03 used a full 3D atmospheric model coupled to an upper mixed ocean layer to derive a linearized operator for sensitivity of the surface heat budget to SST perturbations. The full 3D GCM served as a complicated boundary condition in this setting. A03 interpreted polar amplification as

an intrinsic property of this model as a whole, emerging as a result of excitation of the least stable mode of the linearized surface budget operator. ALB05 used a 'ghost forcing' approach to look for mechanisms that propagate tropical signals to high latitudes. Warmer and moister air propagating to the poles as the climate warms was found to contribute significantly to polar amplification. A similar idea was further developed in LA07 in which a mechanism was offered to explain the polar amplified shape of the least stable mode on an aquaplanet.

Cai (2005) suggested that the atmospheric-dynamic mechanism of PA is tightly linked to the vertical stratification feedback, drawing a parallel between his results and those of Alexeev et al. (2005) concerning significant changes in vertical distribution of temperature as a result of increases in the poleward heat transport from lower latitudes. In a series of more recent articles, further details have been given concerning the interaction between the temperature response and different components of the surface budget (Cai and Lu 2007; Lu and Cai 2009). Graversen and Wang (2009) looked at the sensitivity of a coupled climate model operating in full mode and with locked (prescribed) sea ice. They found that increases in water vapor and cloud cover at high latitudes leads to significant PA in 2 $\times$ CO_2 experiments.

Kay et al. (2012) and Hwang et al. (2011) suggested that total poleward heat transport does not play a significant role in 2 $\times$ CO_2 experiments with different versions of the NCAR coupled model. Their analysis was based on calculations of feedback factors corresponding to various mechanisms operating in the model system. Equilibrium values for AHT and other diagnostics before and after the doubling of CO_2 concentration were used to estimate these feedback values. It was found that AHT does not change significantly as a result of doubling the CO_2 concentration, which led to the conclusion that it does not contribute to polar amplification. Moreover a somewhat negative correlation between the values of AHT change and PA has been found in a suite of IPCC model simulations.

1.3 Scope of the article

As mentioned above, understanding the role played by surface albedo feedback in polar amplification is rather straightforward. This is due to the fact that SAF is easily understood as a positive local feedback. Assessing the contribution of atmospheric heat transport is more difficult due to its dependence on the global circulation. Atmospheric large-scale circulation is greatly variable over a wide range of timescales, which makes it difficult to detect a signal from a small perturbation. In addition, AHT is extremely difficult to prescribe in a full 3D GCM if one wants to separate the effects of circulation on AHT. The AHT consists of several components and each of its individual components introduces additional parameters, further complicating the analysis. Because of these reasons we deliberately chose to use a simplified model in this study.

In this paper we analyze the relative contribution of AHT and SAF to polar amplification using a 2-box EBM. This model is similar to one presented in LA07, but with the addition of active sea ice and exponential dependence of latent heat transport on tropical temperature. We consider several different 'versions' of the model in which certain mechanisms are held fixed and subject them to uniform forcing across a range of climates. We are particularly interested in the effect of AHT on both the equilibrium polar amplification response as well as the dynamics by which the model reaches its new equilibrium.

Subsequent linearization about the present-day climate allows us to compare the timescales of individual model processes via an eigenmode analysis. These timescales, along with corresponding eigenvectors, will control spatial and temporal patterns of model sensitivity. Examples of differences in model behavior with- and without individual feedbacks are compared. In addition, a formal feedback analysis is used to show the relative strengths of model feedback processes both globally and in each box.

2 Description of the model

Figure 1 gives a graphical depiction of the model to be used. It consists of two boxes (tropical and extra-tropical) divided equally area-wise by 30°N latitude. Both boxes receive incoming solar (S_1, S_2) and emit outgoing longwave radiation (OLR_1, OLR_2). The extra-tropical box is partly covered by ice and, hence, reflects a proportional amount of incoming solar radiation. To calculate the ice area we assume the tropical temperature is constant with respect to latitude while the extra-tropical temperature decreases linearly with latitude. This is not an unreasonable assumption given the average meridional temperature profile as described, say, in Peixoto and Oort (1992). The ice-covered area is then defined as the area north of the latitude where the extra-tropical temperature crosses a designated ice margin temperature T_{ice} (chosen here as 271.15 K which is close to the sea ice freezing temperature).

Model equations take the form of an energy balance:

$$\begin{aligned} H\, dT_1/dt &= S_1 - F - (A + BT_1) + \varepsilon \\ H\, dT_2/dt &= S_2(1 - 2\alpha a) + F - (A + BT_2) + \varepsilon \end{aligned} \tag{1}$$

Here H is the upper ocean layer heat capacity; S_1 and S_2 are prescribed net incoming solar fluxes in the tropical and extra-tropical boxes, respectively; A and B are the Budyko-Sellers constants for parametrization of the outgoing long-

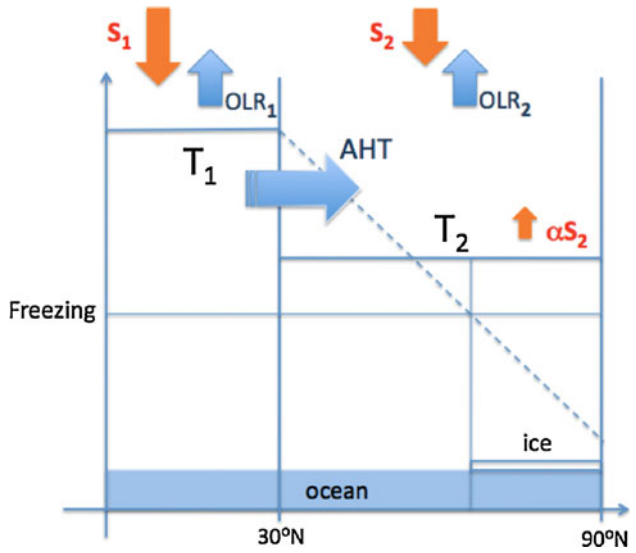

Fig. 1 Model schematics

wave radiation as a function of surface temperature; a is the fractional area of the hemisphere covered by ice; α is the effective ice albedo (difference between ice and land); and ε is the external forcing parameter. Units for these parameters are in petawatts where 1 PW in either box is equivalent to $10^{15}/\pi r^2 = 7.8\ \mathrm{W/m^2}$ at the top of the atmosphere (r is the radius of the earth). The factor of 2 in the second equation is due to the fact that ice area a is given as a fraction of the total hemisphere, hence it must be doubled to account for the ice-albedo effect in the extra-tropical box. As discussed above, the atmosphere is assumed to have minimal heat capacity as compared to the ocean. In any case, for purposes of evaluation of the model, H determines only the relative time scale of the model response, hence precision in the actual value is completely unnecessary.

The atmospheric heat transport F is parameterized as follows:

$$F = F_0 + \gamma_1(T_1 - T_2) + \gamma_2 C(T_1)(T_1 - T_2) \tag{2}$$

$$C(T_1) = 6.11 \exp\left(17.23\frac{T_1 - 273.15}{T_1 - 35.86}\right) \tag{3}$$

The first term in this formula for F describes the mean background value; the second and third terms are included to mimic the sensible and latent heat transports, respectively. Exponential dependence of latent heat transport on T_1 describes the moisture availability in the atmosphere. The particular form given is that of the Magnus-Tetens approximation to the Clausius-Clapeyron equation which takes into account the temperature dependence of the latent heat of vaporization at the phase-change boundary (Murray 1967). We have assumed that the majority of the moisture in the extra-tropical free atmosphere comes from the tropics and therefore we do not include T_2 in the expression for $C(T_1)$. Analysis of the case when coefficient C depends on both T_1 and T_2 was done ion LA07 and it was shown that the results do not change in a qualitative sense.

The latitude of the ice margin, ϕ_{ice}, is determined geometrically as mentioned above:

$$\phi_{\mathrm{ice}} = 30^\circ + 30^\circ(T_1 - T_{\mathrm{ice}})/(T_1 - T_2). \tag{4}$$

Moreover, the ice area as a fraction of the hemisphere depends on ϕ_{ice} as follows:

$$a = 1 - \sin(\phi_{\mathrm{ice}}). \tag{5}$$

We constrain this area to realistic values in the model by assuming that the latitude of the ice margin cannot be lower than 30°N or higher than 90°N. However, the ice cap never approaches 30°N for the range of climates we consider in this article.

The model is tuned to reproduce a 'present-day-like' climate with respect to observed mean temperatures, ice area, and heat transport at 30°N. The parameters used to achieve this present-day model climate are given in Fig. 2.

The model described here is similar to the energy balance model used in LA07 except that we have added surface albedo feedback and slightly modified the latent heat terms. The model represents a rather standard set of processes and has no essential novelties. The relative roles of sensible and latent heat flux contributions to the total AHT are controlled by values γ_1 and γ_2. They are chosen so that near the present-day climate the total AHT remains fairly constant under uniform forcing. Some values and units used in the model may look arbitrary. E.g. we chose a value for B equivalent to $2.22\ \mathrm{W/m^2}$, which corresponds to a 'clear sky' emissivity as described in Budyko (1969). Actual values of model parameters will have no physical meaning in such a simple setting. We do not view this as a

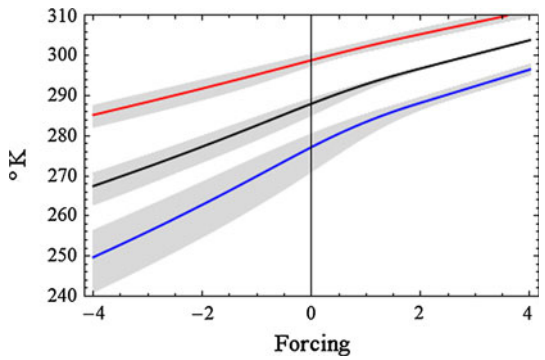

Fig. 2 Model climates. Horizontal axis gives the TOA forcing. Specific values for model parameters are: $S_1 = 40.9$ PW; $S_2 = 24.1$ PW; $\alpha = 0.29$; $A = -49.7$ PW; $B = 0.29$ PW/K; $F_0 = 3$ PW; $\gamma_1 = 0.035$; $\gamma_2 = 2.852$. *Grey bands* show the total effect on temperatures of allowing independent 10 % variation in the values for α, γ_1, and γ_2

major problem because our main goal is to qualitatively assess the relative importance of atmospheric heat transport for the dynamics of global warming.

3 Climate sensitivity over a range of climates

In order to study sensitivity of our model to $2 \times CO_2$ forcing we first obtain a set of equilibrium climates from very cold to very warm. Climates are obtained by simply applying a uniform TOA forcing of different magnitudes (from -4 to $+4$ PW) and running the model to equilibrium.

Figure 2 shows equilibrium model climates plotted against forcing parameter with forcing value 0 corresponding to a present-day-like climate. Also shown are gray bands which describe the effect of independent 10 % variation of the parameters α, γ_1, and γ_2.

Figure 3 shows total AHT plotted against forcing along with the variations in AHT which result from perturbation of key parameters. One thing we notice from 3 is that total AHT response to forcing is rather flat in the 'present-day' climate and is even seen to decrease somewhat in response to forcing. Moreover, this flatness remains relatively unchanged upon perturbation of parameters controlling AHT flux (γ_1, γ_2). On the other hand, the slope of the heat transport flux in the 'present-day' climate seems mostly determined by ice albedo (α).

A similar phenomenon shows up in Fig. 4 which shows the change in AHT due to forcing normalized on the forcing value. As the figure indicates, unless the value of the ice albedo is perturbed too far, then there is very little change in AHT due to forcing in the 'present-day' climate and, moreover, this behavior does not seem to be very much affected by variations in the parameters controlling AHT flux.

Figure 5 shows the polar amplification obtained by subjecting the model climates to a small positive forcing. Polar amplification is calculated at each equilibrium state by applying an incrementally small uniform forcing, dividing the resulting temperature changes in the extratropical and tropical boxes, respectively. As in Fig. 3, we show sensitivity of PA to variation of parameters. As Fig. 5 makes clear, the polar amplified response of the model is shaped by both SAF and AHT processes. Also, in all but the warmest climates the polar amplified response of the model shows the most sensitivity to the ice albedo parametrization.

4 Contribution of AHT and SAF to polar amplification

From this point on we fix α, γ_1, and γ_2 at the values given in Fig. 2. These are the median values shown in Figs. 3, 4 and 5. As noted above, with these values a small positive forcing applied in the present-day climate will result in a negligible change in total AHT (though not, of course in its sensible and latent heat components). This is done intentionally and is in line with recent studies using more complex GCMs such as Hwang et al. (2011), and Kay et al. (2012).

In order to assess the relative roles played by SAF and AHT in contributing to PA, we run our model in three different cases: (1) all feedbacks operating, (2) SAF turned off, and (3) AHT feedback turned off. Figure 6 shows the resulting polar amplification in each of these cases.

One can see that the model will always show polar amplification in two cases: when all feedbacks are operating and when SAF is turned off. For the case where there is no AHT feedback, the model shows polar amplification only when there is positive ice area. Not surprisingly, when sea ice disappears, polar amplification values coincide in cases 1 (all feedbacks) and 2 (no SAF). Also, not surprisingly, the model response exhibits no polar amplification when sea ice disappears in case 3 (no AHT feedback).

AHT behavior for cases 1 and 2 is illustrated in Fig. 7. Shown are changes in AHT as a result of applying a small uniform forcing normalized on the forcing value over a range of equilibrium climates (cf. Fig. 4). When SAF is turned off (case 2, blue dashes) the increase in AHT is uniform across all climates. We conclude that the decrease in sensible heat flux due to the polar amplified response (case 2, Fig. 6) is offset by a greater contribution from the

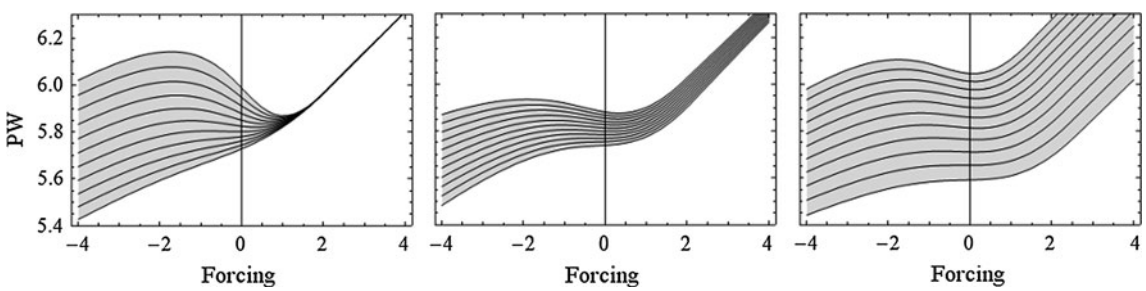

Fig. 3 Total AHT in PW (common scale) plotted against forcing. *Each panel* shows the effect of 10 % variation of individual parameters α (*left*), γ_1 (*center*), and γ_2 (*right*)

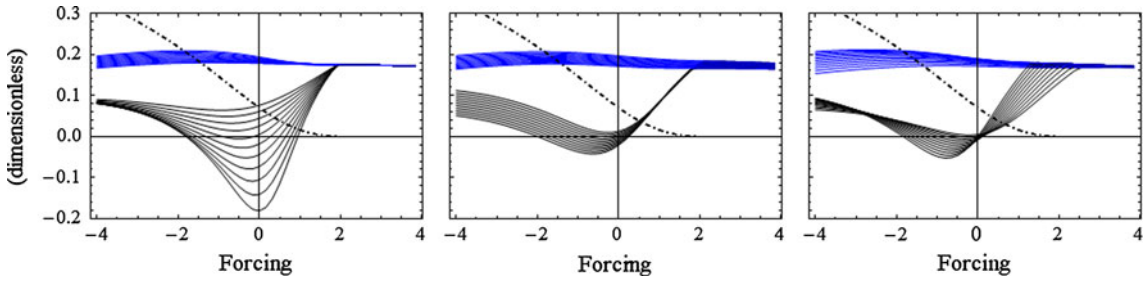

Fig. 4 *Dark lines* show change in total AHT due to small positive forcing, normalized on the forcing value in the full model over the range of model climates. Additionally, *each panel* shows the effect of 10 % variation of individual parameters α (*left*), γ_1 (*center*), and γ_2 (*right*). *Blue lines* show the normalized change in AHT in a particular submodel in which there is no ice albedo feedback (i.e., ice area is held fixed at the equilibrium value)

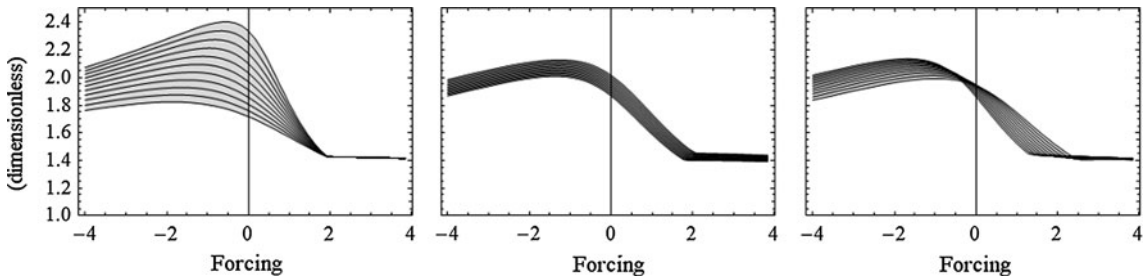

Fig. 5 Polar amplification $\Delta T_2/\Delta T_1$ plotted against forcing. *Each panel* shows the effect of 10 % variation of individual parameters α (*left*), γ_1 (*center*), and γ_2 (*right*)

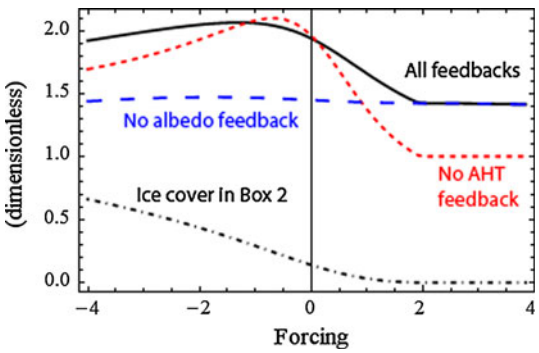

Fig. 6 Polar amplification $\Delta T_2/\Delta T_1$ plotted against forcing in three different cases: all feedbacks operating (case 1, *solid line*), SAF turned off (case 2, *long dashes*), and AHT feedback turned off (case 3, *short dashes*). Also shown is the fractional area of ice in box 2

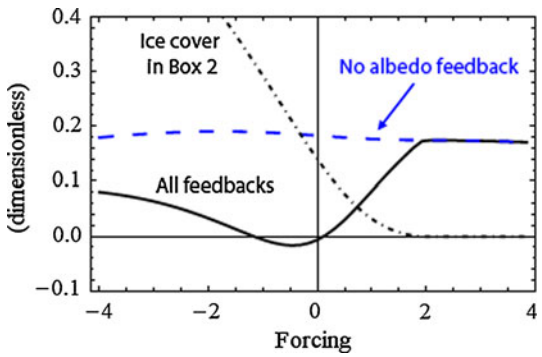

Fig. 7 Change in total AHT due to forcing, normalized on the forcing value

latent heat component because there is more moisture in the system when the climate is warmer.

However, when SAF is active the AHT behavior is quite different (case 1, solid line, Fig. 7). In this case, the total AHT change in response to a uniform forcing is negligible near the present-day climate and is small overall when compared to case 2 until sea ice starts disappearing. We conclude that the greater polar amplified response in case 1, which includes both AHT feedback and a strong ice albedo response, leads to a more or less equal change in latent and sensible fluxes of opposite sign. In this way the total AHT remains more or less constant near the present-day climate. This is the primary reason why the polar amplification of the full model and the model with fixed AHT coincide near the present-day climate and diverge significantly as the climate warms. When sea ice area is small, the albedo feedback becomes less important and the only mechanism left to produce polar amplification is AHT.

The small variation in equilibrium AHT for climates near the present-day has several interesting consequences for the polar amplification exhibited in the model. The first is that polar amplification may be given in terms of the ice response to forcing. In particular, if ε represents a uniform forcing applied to the model equations, then assuming the

heat transport term F does not change under uniform forcing we can calculate the equilibrium temperature change in each region as

$$\begin{aligned}\Delta T_1 &= \varepsilon/B \\ \Delta T_2 &= \varepsilon/B - 2\alpha S_2 \Delta a/B\end{aligned} \tag{6}$$

where Δa is the change in ice area due to forcing. Therefore, we obtain the the polar amplification due to a uniform forcing as follows:

$$\frac{\Delta T_2}{\Delta T_1} = 1 - 2\alpha S_2 \Delta a/\varepsilon \tag{7}$$

This shows that AHT does not contribute to polar amplification for climates in which there is no change in AHT in response to forcing. Indeed, in such instances there is no difference between the full model (case 1) and the model in which AHT is held constant (case 3).

However, there is another expression for the polar amplified response of climates near the present-day which is intriguing for its sole dependence on the AHT term F. Namely, if $F = F(T_1, T_2)$ is the flux term given by Eq. (2), then for climates in which $dF/d\varepsilon = 0$ we have

$$0 = \frac{dF}{d\varepsilon} = \frac{\partial F}{\partial T_1}\frac{dT_1}{d\varepsilon} + \frac{\partial F}{\partial T_2}\frac{dT_2}{d\varepsilon} \tag{8}$$

so that polar amplification may be given by

$$\frac{\Delta T_2}{\Delta T_1} = -\frac{\partial F}{\partial T_1}\Big/\frac{\partial F}{\partial T_2} \tag{9}$$

This expression is interesting in that it applies to any formulation of the flux term, not just the particular one given by Eq. (2). Moreover, it describes the polar amplification of the full model in terms of the functional expression of a particular component—a component which we have just seen plays seemingly no role in shaping the polar amplified response! This issue is discussed further in Sect. 6.

The fact that SAF is the dominant feedback for climates near the 'present-day' climate should be viewed with caution as this could be a mere coincidence. The important point here is the fact that there is a potential for SAF to play the leading role in forming the PA response to a uniform forcing. Moreover, this will be the case for climates in which there is no change in AHT in response to forcing.

On the other hand, SAF need not be the sole contributor to polar amplification, or even the most dominant one. Obviously, there can be no polar amplification due to SAF for the two extremes in which the model forms no ice or the ice cap reaches maximum extent. However, Fig. 6 shows that the decline in polar amplification due to SAF alone occurs well before the disappearance of the ice cap. This occurs simultaneously with a divergence of the polar amplification curves for cases (1) and (3) due to the increasingly positive AHT response to forcing in warmer climates shown in Fig. 7.

5 Feedback analysis

One can apply a standard feedback analysis to quantify the effects of different model components. At a given climate we force different versions of the model and compare the relative responses. Namely, for a given feedback process β, we let ΔT_β measure the response of the model in which β is the only feedback process operating. Following the discussion in Peixoto and Oort (1992), if ΔT_0 measures the response of the base model with all feedbacks turned off, then the feedback parameter f_β is defined as follows:

$$f_\beta = 1 - \Delta T_0/\Delta T_\beta \tag{10}$$

If the system gain due to the feedback β is $G_\beta = \Delta T_\beta/\Delta T_0$, then we arrive at the familiar equation

$$G_\beta = (1 - f_\beta)^{-1} \tag{11}$$

In Fig. 8 we plot surface albedo and AHT feedback parameters calculated with respect to the global temperature $T_{\text{avg}} = (T_1 + T_2)/2$. For comparison, we also show the global feedback parameter $f = 1 - \Delta T_0/\Delta T$, where ΔT is the response of the model with all feedbacks turned on.

This figure clearly illustrates that SAF is the only apparent feedback with respect to the mean global temperature response. Indeed, the AHT feedback is nearly zero in all climates and so, from the point of view of a formal feedback analysis based on global temperature response, AHT appears completely unimportant. The reason for this, of course, is the fact that individual changes in the two boxes induced by the applied forcing cancel out due to conservation of energy when calculating the global temperature. Because of this, if we want to account for the role

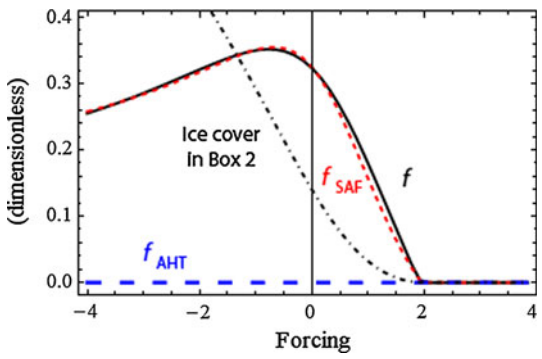

Fig. 8 Feedback parameters f, f_{SAF}, and f_{AHT} calculated with respect to global average temperate over a range of climates/forcings. *Red, dashed* = SAF; *blue, long dashes* = AHT feedback; *black, solid* = global feedback parameter. Ice area in box 2 is also shown (*dot-dashed*)

AHT plays in the global temperature distribution—and thereby, polar amplification—we will obviously need to carry out a similar feedback analysis for individual boxes.

5.1 Feedbacks in individual boxes

Figure 9 shows feedback parameters calculated by formally applying Eq. (10) to temperatures in individual boxes. From this figure we see that both SAF and AHT act as positive feedbacks in the extra tropics (box 2). For the present-day climate the strength of the extra-tropical surface albedo feedback is more than twice as strong as that of the AHT feedback. However, it is also clear that extra-tropical SAF begins to decrease from the present-day climate as the ice cap recedes. Because of this, as the climate warms the AHT feedback becomes more important relative to SAF. Eventually, in very warm climates, AHT is the dominant feedback in the extra-tropics.

Also clear from Fig. 9 is the fact that ice albedo feedback is not a feedback at all when considering tropical temperatures. Of course, this is due to the fact that there is no ice in the tropics and hence no ice-albedo response to forcing. AHT, on the other hand, is seen to act as a sizable negative feedback in the tropics.

In a standard feedback analysis similar to that described above, it is assumed that feedback processes are arranged 'in parallel' and that each individual process feeds a fixed fraction of the system output back into the system input. In this way, the total feedback parameter for the full system can be expressed as the sum of the individual feedback factors. This is precisely what we see in our model for the case of feedbacks calculated relative to mean global temperatures (Fig. 8). However, this is no longer the case when we calculate feedbacks in individual boxes. This can be seen in Fig. 10 where we plot $f - f_{\mathrm{SAF}} - f_{\mathrm{AHT}}$ for both regions.

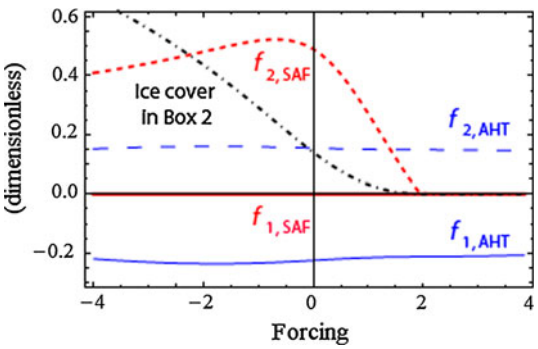

Fig. 9 Feedback parameters f, f_{SAF}, and f_{AHT} for individual processes in the tropics and the extra-tropics plotted against TOA forcing. *Red, solid* = tropical SAF; *red, dashed* = extra-tropical SAF; *blue, solid* = tropical AHT feedback; *long blue dashes* = extra-tropical AHT. Also shown in ice area in box 2 (*dot-dashed*)

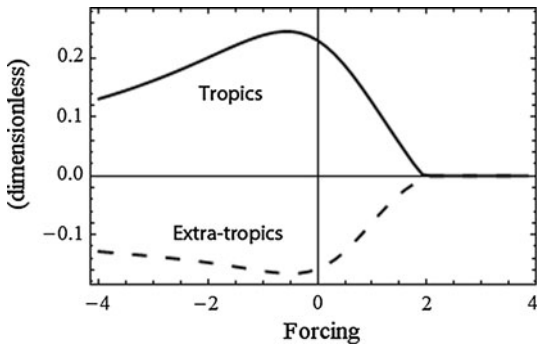

Fig. 10 Difference between global and individual feedback parameters in different boxes. *Solid* = tropics; *Dashed* = extra-tropics

What Fig. 10 shows is that on the level of individual boxes the feedback of the full model (with all feedback processes turned on) cannot be calculated simply by summing the feedback factors of individual processes. This is due to the fact that the magnitude of the signal fed back into an input by a given process, say AHT feedback into box 1, depends not only on the output of box 1, but also on the output of box 2.

Because of this, it is instructive to consider the effect a given feedback process has on the full model while allowing for interactions with other feedback processes.

5.2 'Top-down' feedback analysis

Rather than determine the effect a single feedback process has on a base model with all feedbacks turned off, let us consider instead the effect a single process has on the model when all other feedbacks are turned on.

To this end, consider the quantity

$$\frac{\Delta T}{\Delta T_{\mathrm{SAF}}} = \frac{1 - f_{\mathrm{SAF}}}{1 - f} = \left(1 - \frac{f - f_{\mathrm{SAF}}}{1 - f_{\mathrm{SAF}}}\right)^{-1} \tag{12}$$

which can be calculated either globally or in individual boxes and which represents the system gain of the full model over the model with no AHT feedback. Comparing Eqs. (11) and (12), we conclude that the quantity

$$f^*_{\mathrm{AHT}} \stackrel{\mathrm{def}}{=} \frac{f - f_{\mathrm{SAF}}}{1 - f_{\mathrm{SAF}}} \tag{13}$$

is a 'feedback factor' for AHT over a 'base model' in which all processes are operational except AHT. Hence, this 'top down' feedback parameter f^*_{AHT} essentially measures the feedback effect of AHT in the full model. The corresponding feedback factor for SAF is

$$f^*_{\mathrm{SAF}} \stackrel{\mathrm{def}}{=} \frac{f - f_{\mathrm{AHT}}}{1 - f_{\mathrm{AHT}}}. \tag{14}$$

These quantities are shown over a range of climates in Fig. 11.

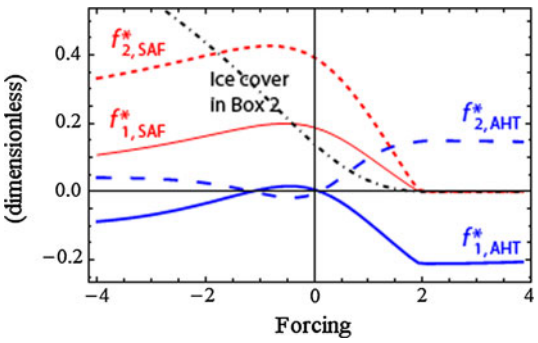

Fig. 11 Feedback factors f^*_{SAF} and f^*_{AHT} in both tropical and extra-tropical regions. *Solid lines* are tropics, *dashed lines* are extra-tropics

It is apparent from Fig. 11 that SAF remains a strong positive feedback in the extra-tropics. However, the figure also shows that SAF acts as a positive feedback in the tropics as well. This is in contrast to Fig. 9 where SAF did not act as a feedback at all in the tropics. The point, of course, is that SAF does have a destabilizing effect on the tropics in the full model. However, AHT is the mechanism by which this effect is realized: when the extra-tropical temperature rises faster than the tropical temperature (because of SAF) the heat transport between the boxes decreases thus making the tropical temperature increase. Because of this, the tendency of SAF to destabilize tropical temperatures will not be observed in a standard feedback analysis where the effect of SAF is assessed with AHT being switched off.

Concentrating now on f^*_{AHT}, Fig. 11 shows a distinct contrast with Fig. 9. Whereas in Fig. 9 AHT was shown to act as a substantial feedback in both regions, in Fig. 11 we see that AHT feedback is negligible (or reduced by an order of magnitude) over a 10 K interval near the present-day climate. That is to say, for the 'present-day' climate climate (that is, the model climate according to our simple model), AHT does not seem to operate as a significant feedback process in either region when the surface albedo feedback is operational. We might say, then that while AHT is a substantial feedback over a range of climates in the usual sense (over a base climate with no feedbacks), surface albedo feedback has the potential in certain climate scenarios to suppress or restrict the ability of AHT to act as a feedback in the full model. However, even in these scenarios the composition of the heat transport term will change to include less sensible and more latent heat transport, bringing more moisture in the air to high latitudes and resulting in potentially significant changes to 'local' radiative and cloud-feedback processes.

Of course, the ability of local processes to mask the AHT feedback effect is not guaranteed in all climate scenarios. For our simple model, this occurs only near the present-day climate. As the strength of the surface albedo feedback diminishes (in either very warm or very cold climates) the AHT feedback becomes increasingly important. Indeed, outside the present-day climate AHT feedback increasingly works as a destabilizer on the extra-tropical box and as a stabilizer on the tropical box. As sea ice area decreases to zero the AHT feedback parameters return to the values given in Fig. 9.

One important conclusion that can be drawn from this discussion is that formal feedback analysis applied to the global temperature will not reveal the significance of the AHT feedback, even when SAF is absent. Feedback analysis for individual boxes is needed. Another conclusion is that when active, SAF may result in reduced variability of total AHT response to forcing (Fig. 7) and hence reduce the feedback effect of AHT (Fig. 11) so that the AHT feedback does not participate significantly in shaping the global warming response. This could well be the case for our present-day climate which is located near the maximum feedback value for SAF in Figs. 8, 9, and 11. Our analysis does suggest, however, that AHT feedback may start playing a more explicit and prominent role in shaping the warming response in our current climate with disappearing sea ice. The physical mechanisms involved in shaping this response are discussed below.

6 Temporal response to forcing

In this section we concentrate primarily on the behavior of our model in the present-day climate. By 'present-day climate' we mean a climate with global mean temperature near 288 K, a total poleward heat transport at 30°N of about 6 PW, and sea ice margin at some intermediate position around 60−70°N so that ice-albedo feedback is active.

As the discussion above shows, we may choose present-day climates and small positive forcings such that the total atmospheric heat transport at equilibrium will not change when the model is forced (see Fig. 7). Hence, the equilibrium temperature response for the model with fixed AHT will be identical to that of the full model when subjected to the chosen small uniform forcing. However, both the composition of the AHT (latent vs. sensible) as well as the transient response of the models will be different. It is this transient response to forcing that we focus on in this section.

6.1 Instantaneous and gradually forced 'global warming' experiments

Figure 12a shows phase diagrams (ΔT_2 plotted against ΔT_1) of three model versions when subjected to uniform instantaneous forcing: the full model with all feedbacks

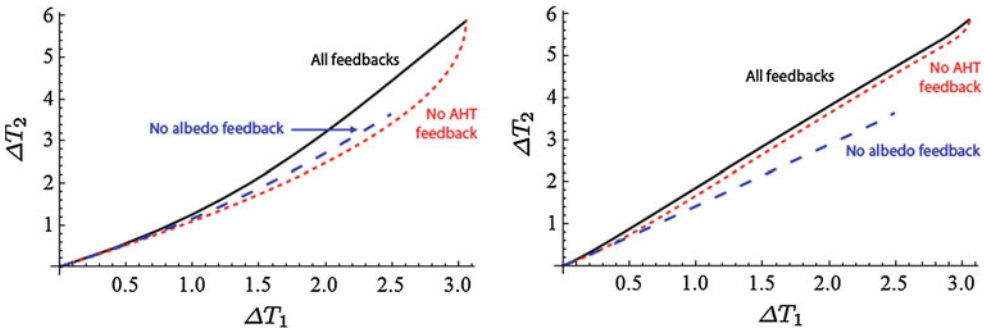

(a) Instantaneous forcing **(b)** Gradual forcing

Fig. 12 Phase diagram (ΔT_1 vs. ΔT_2) of three model versions subjected to instantaneous (**a**) and gradual (**b**) uniform positive forcing. Movement in time is to the upper right. *Solid black* = all feedbacks; *long blue dashes* = fixed SAF; *short red dashes* = fixed AHT

operating, one in which AHT is fixed, and one in which ice area is fixed. For a point on any given curve, the PA of the corresponding climate state is given by the slope of the line that connects this point to the origin. As Fig. 12a shows, PA for the full model remains nearly constant throughout the entire response interval. The same is true for the model in which SAF is held constant. However, the situation is different for the model in which AHT is held constant. In this case, the climate does not reach its full PA until late in the response interval.

One point to emphasize here is that the simplicity of our model allows us to distinguish between the responses of the 'all-feedback' and 'no-AHT-feedback' cases when subjected to uniform forcing. Moreover, the two trajectories in Fig. 12a would need to coincide if the AHT was not important in shaping the model response. Variability on all time scales and noise, which are inevitably present in more complicated models, are likely to make detection of this difference more difficult.

One question that arises is whether or not this behavior is robust with respect to the manner in which the forcing is applied. For instance, applying forcing gradually (e.g., linear over some time interval), results in the phase diagram given in Fig. 12b. In this figure we see that the phase plots for the full model and the model with fixed AHT have nearly converged. That is, the models equilibriate over an identical range of climate states.

At first glance this might seem to indicate that AHT is not important for shaping the warming response of the model to uniform gradual forcing. However, a visual comparison of the phase diagrams alone does not give a very good picture of the rates at which the climates evolve. Indeed, when we plot PA as a function of time (Fig. 13) we see that the qualitative behavior of the model response is the same in both scenarios: the model in which AHT is fixed evolves on a longer timescale than the full model regardless of how the forcing is applied. While this difference for the gradually forced scenario is not detected in a comparison of phase plots, it is nevertheless seen in the PA time series.

This difference in response to forcing in the 'all-feedback' and 'no-AHT-feedback' model versions can be attributed to the fact that in the full model there is a transient AHT response (shown in Fig. 14) that leads to increased heat transport in a warming scenario. The areas under the curves in Fig. 14 are equal in both forcing scenarios and serve as a measure for the amount of energy withdrawn from box 1 in the equilibration process. This AHT response causes the temperatures in both boxes to converge to their new equilibria at more or less similar rates. For the model in which AHT is kept fixed there is no such transient response and, as a result, T_1 will converge to its equilibrium faster than T_2.

The maximum AHT anomaly is relatively small in the instantaneously forced case (about 0.1 PW) and it is an

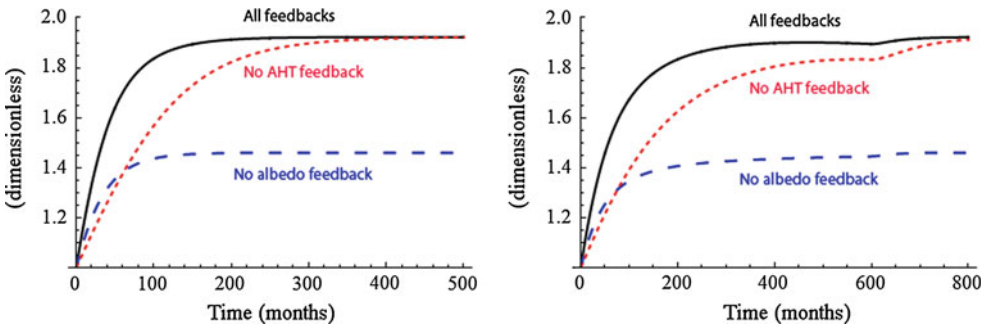

(a) Instantaneous forcing **(b)** Gradual forcing

Fig. 13 Polar amplification ($\Delta T_2/\Delta T_1$) plotted against time for **a** uniform instantaneous and **b** uniform gradual forcing. *Solid black* = all feedbacks; *long blue dashes* = fixed SAF; *short red dashes* = fixed AHT. Gradual forcing was applied linearly over 50 model years (600 months)

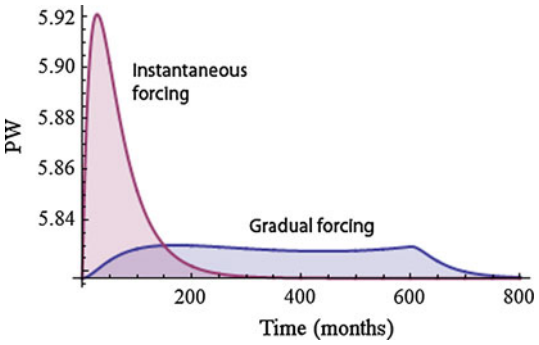

Fig. 14 Transient AHT response to uniform instantaneous and gradual forcing. The areas under both curves (i.e., the total poleward energy transport) are identical

order of magnitude smaller for the gradually forced case. As such, they both would be hard to detect in a 'realistic' model with all the variability typical for large climate models. But again, the AHT will withdraw the same amount of energy no matter how slowly we apply the forcing.

We should note, again, that these experiments were run near the present-day climate which is located near a maximum SAF value (Fig. 9) and a local minimum AHT (Fig. 7). Indeed, the point of this discussion is to examine the impact of AHT even when its equilibrium value does change under forcing. If, however, we run these same experiments in different climates where the total AHT does change under forcing, then we will see increased differences in model versions, including their equilibrium polar amplified response (Fig. 6).

6.2 Model timescales and adjustment to equilibrium

In this section, we consider the characteristic timescales of individual model processes as a way to explain the differences in equilibration trajectories as described above. We will see that SAF acts over a longer timescale than both AHT feedback and top-of-atmosphere radiation. Thus, by keeping AHT fixed, the extra-tropical box is forced to equilibrate along the slower SAF and TOA timescales.

Let $\overline{T}_i$ denote the equilibrium temperature of region i in the present-day climate and $T_i' = T_i - \overline{T}_i$ the perturbation from equilibrium, then we can rewrite the model equations (1) in the following linearized form:

$$H\begin{bmatrix} dT_1'/dt \\ dT_2'/dt \end{bmatrix} = J\Big|_{(\overline{T}_1,\overline{T}_2)} \cdot \begin{bmatrix} T_1' \\ T_2' \end{bmatrix} + \varepsilon. \tag{15}$$

The final term in this equation represents a uniform forcing

$$\varepsilon = \begin{bmatrix} \varepsilon \\ \varepsilon \end{bmatrix} \tag{16}$$

and J is the Jacobian derived from the model equations:

$$J = \begin{bmatrix} -B - \partial_{T_1}F & -\partial_{T_2}F \\ \partial_{T_1}(F - 2\alpha S_2 a) & -B + \partial_{T_2}(F - 2\alpha S_2 a) \end{bmatrix} \tag{17}$$

To solve for the steady state temperature perturbations we set the time derivatives to zero and solve:

$$\begin{aligned} \begin{bmatrix} T_1' \\ T_2' \end{bmatrix} &= -J^{-1}\Big|_{(\overline{T}_1,\overline{T}_2)} \cdot \varepsilon \\ &= \frac{\varepsilon}{\det\,(J)} \begin{bmatrix} B - 2\partial_{T_2}(F - \alpha S_2 a) \\ B + 2\partial_{T_1}(F - \alpha S_2 a) \end{bmatrix} \end{aligned} \tag{18}$$

At this point Eq. (18) can be used to give expressions for mean global temperature change after forcing as well as the ratio between warming at high and low latitudes (i.e., polar amplification). For present-day parameters we obtain a global sensitivity of 0.67 K/W/m^2, which is well within the range predicted by IPCC models (see also Forest et al. 2002). Polar amplification in the linear model is independent of forcing magnitude and has a value of 1.96 in the present-day. This is in line with values of present-day PA exhibited by the full model (Fig. 6).

Additionally, by setting the appropriate terms to zero in Eq. (18) we can find values for global sensitivity and PA of model versions in which AHT and SAF are fixed at equilibrium values. Obviously, an analysis of this kind cannot describe non-linearities that occur when we subject the full model to large forcing, let alone when the model jumps to another branch of the multi-equilibrium solution curve. By applying a linear framework we can only analyze small changes for a given climate.

To find the characteristic timescales of individual model processes, consider the two 'submodels' or specializations of the full linear model in which (1) SAF is fixed at the equilibrium value and (2) AHT is fixed at the equilibrium value. Each of these two specializations have a common eigenvalue, $-B/H$, determined by TOA processes. In fact, this is the same TOA eigenvalue exhibited in Langen and Alexeev (2007) and is determined by the heat capacity of the system and the rate at which excess energy can be emitted to space. The corresponding eigenvectors are found to be:

$$\text{TOA eigenvector, fixed SAF} = \begin{bmatrix} -\partial F/\partial T_2 \\ \partial F/\partial T_1 \end{bmatrix} \tag{19}$$

$$\text{TOA eigenvector, fixed AHT} = \begin{bmatrix} -\partial a/\partial T_2 \\ \partial a/\partial T_1 \end{bmatrix} \tag{20}$$

The TOA eigenmode has a characteristic timescale of $H/B = 2.9$ year in both model versions. Clearly this quantity is greatly determined by our choice of upper ocean layer heat capacity H, the accuracy of which we argued in Sect. 2 is immaterial to our discussion. This is still the case here since it is not the absolute timescale we are interested in, but rather a comparison of the timescales related to individual model processes.

The eigenvector for the model version in which SAF is fixed is seen to have a polar amplified form of magnitude

$$\frac{\Delta T_2}{\Delta T_1} = -\frac{\partial F}{\partial T_1} \Big/ \frac{\partial F}{\partial T_2}.$$

This is the same expression for PA which we obtained in Eq. (9) under the assumption that equilibrium AHT remains constant under forcing. Indeed, this quantity shows good agreement with PA derived from the full model (from Fig. 6) precisely in the present-day climate regime in which we have seen there is little change in equilibrium AHT values in response to forcing (see Fig. 15).

On the other hand, for the model version in which AHT is fixed, the TOA eigenmode is one of equatorial amplification of magnitude:

$$-\frac{\partial a}{\partial T_2} \Big/ \frac{\partial a}{\partial T_1} = \frac{T_1 - T_{\text{ice}}}{T_2 - T_{\text{ice}}}.$$

Of course, TOA is not the only active process. Indeed, each model version has a second eigenmode which corresponds either to AHT or SAF, depending on which processes are held fixed. The non-TOA eigenvector for the model with fixed SAF is [−1,1] (that is, one of pure heat transport between regions). This mode is found to have characteristic time scale

$$\frac{H}{B + \partial F/\partial T_1 - \partial F/\partial T_2}.$$

This is approximately 1.25 year for 'present-day' conditions. Hence, pure heat transport between regions represents the fast mode in this model.

For the model version in which AHT is fixed, the non-TOA eigenvector is seen to be [0,1] with a corresponding characteristic timescale

$$\frac{H}{B + 2\alpha S_2 \partial a/\partial T_2}.$$

This quantity is approximately 6.6 year in the present-day. Hence, this eigenmode is one of strict polar amplification and represents the slow mode in the model.

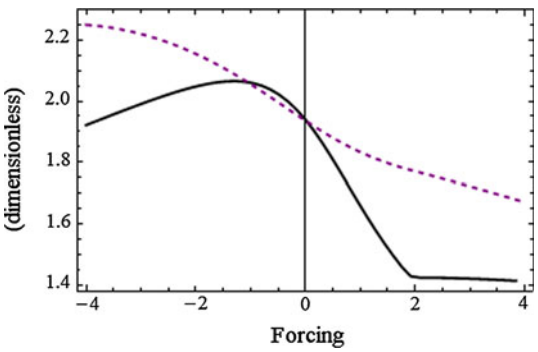

Fig. 15 Polar amplification in the full model (*solid line*) compared to $-(\partial F/\partial T_1)/(\partial F/\partial T_2)$ (*dashed line*)

Because different versions (or submodels) will have different eigenmodes and timescales, we see that fixing sensitivities in expressions for AHT and SAF can result in significant changes in temporal model response. This can be nicely illustrated by comparing submodel relaxation trajectories after temperature perturbation. Again, we choose a 'present-day' climate in which AHT does not change in response to a small uniform external forcing. Figure 16 shows relaxation trajectories after three model versions are given temperature perturbations from the common equilibrium. One can see that the behavior is quite different depending on which model version is used. In particular, the full model relaxation trajectories are closest to those of the 'fixed-SAF' model version in which only AHT is allowed to vary. We believe that this is because the fast AHT mode plays a larger role in shaping the full model response than the slower SAF and TOA processes. Indeed, the fast mode in the full model is found to have a characteristic timescale of 1.3 year, which is nearly identical to the fast mode of the 'fixed-SAF' model version.

A similar experiment was conducted in LA07 to calculate the least stable mode of the system. That same least stable model was found to be primarily responsible for shaping the PA response in a 2 × CO_2 experiment.

7 Discussion, conclusions

In this study, we have used a simple energy balance model to assess the roles of SAF and AHT in shaping the polar amplified response to uniform forcing. A simple model was chosen intentionally in order to be able to fix individual mechanisms responsible for polar amplification in the model. Fixing the atmospheric heat transport is not easy in a full 3D GCM in a physically justified manner. Prescribing surface albedo feedback is not as simple as it may sound either. We argue that our model's behavior captures the big picture as it describes important processes responsible for polar amplification.

The subject of SAF versus AHT feedback has been a lively topic in the polar amplification debate recently. Surface albedo feedback has long been considered the dominant process contributing to polar amplification. However many studies have demonstrated the importance of AHT and other processes in shaping the polar amplified response in models without surface albedo feedbacks (Flannery 1984; Schneider et al. 1997; Alexeev 2003; Rodgers et al. 2003; Alexeev et al. 2005; Langen and Alexeev 2005a, b; Cai 2005; Langen and Alexeev 2007; Graversen and Wang 2009). On the other hand, several recent articles make the case that AHT plays little role in contributing to PA in fully coupled models with all feedbacks active (Kay et al. 2012; Hwang et al. 2011). Hence,

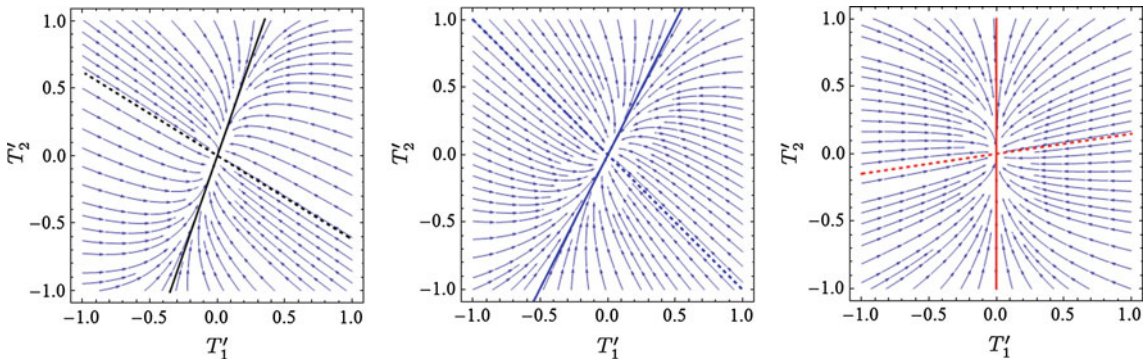

Fig. 16 Relaxation trajectories (T'_1 vs T'_2) after temperature perturbation in submodels: full model (**a**), fixed SAF (**b**), and fixed AHT (**c**). *Dotted lines* represent eigenvectors of the respective fast modes, *solid lines* are eigenvectors of slow modes

the main idea of our article was to analyze the interaction between SAF and AHT feedbacks in a simple model incorporating the key features of both processes. Conceptual estimates of how major mechanisms can impact climate sensitivity are sometimes viewed as too simplistic, although they often provide valuable insights of didactic nature. However, as the foregoing analysis demonstrates, our simple model provides an example of how polar amplification can depend on the relative strength of, and interaction between SAF and AHT feedbacks in different climates. Further, our analysis shows how the presence of AHT can shape the full model's transient response to forcing even when total AHT remains unchanged in the equilibrium.

Consistent with many previous studies including those using full 3D GCMs, we find that an active AHT response will lead to significant polar amplification in fixed ice cap scenarios. On the other hand, we show that an active surface albedo feedback tends to mask the amplifying effect of AHT over a wide range of climates close to that of the present-day. Interestingly, this tendency is not revealed in a standard feedback analysis in which the effect of an individual process is measured against a base system with no active feedbacks. This is because the effect a given feedback process has on the temperature of a single box depends on the output from both boxes. Because of this, we suggest a 'top-down' analysis that considers the effect a given process has on the full model. According to this approach, when SAF is turned off, AHT is seen to act as a substantial feedback across a wide range of climates. Yet once we allow SAF to freely adjust to changes in climate the feedback effect of AHT drops significantly in climates close to the present-day.

Because of this we examine present-day climates in which certain positive forcings result in no change to the total AHT at equilibrium. In such cases AHT plays no role, by definition, in shaping the equilibrium warming response. However, a closer analysis shows that AHT does play a part in determining the trajectory by which the climate adjusts to its new equilibrium. In models with active AHT there will be a transient increase in poleward heat flux which leads to equilibration of both boxes at more-or-less equal rates. By fixing AHT, the boxes will instead adjust independently according to the slower TOA and SAF timescales.

The atmospheric heat transport in a new equilibrium does not have to change in order to produce polar amplification in response to a global uniform forcing with active surface albedo feedback. However, a transient increase in AHT in response to forcing will contribute to the manner in which the equilibrium PA is reached by extracting more heat from the tropics and depositing it in the extra tropics. This process withdraws a significant amount of energy from the tropics independently of the manner in which the external forcing is applied (instantaneous or very gradual) leading to faster equilibration of the model.

There are many other factors and mechanisms that are potentially very important contributors to polar amplification which are not present in our model, including clouds and atmospheric vertical stratification. However, common sense dictates that the relative complexity of all physical processes included in a model should be reasonably balanced. For example, one should not look for explanations of 'baroclinic nature' from a single level barotropic vorticity equation. Therefore including effects of, for example, change in vertical stratification in a model with two slabs—one for the atmosphere and one for the ocean—would overload the system with physics that could not be supported by the dynamics in its present simplified form. Additionally, while our ocean in its present 'slab' form still captures zero order effects of delayed ice formation because of ocean memory, the addition of an 'active' ocean transport would modify the behavior of the heat budget in both boxes. Analysis of these factors is outside the scope of this article, however.

This study was devoted only to experiments with a uniform forcing. An important aspect of the story is that atmospheric heat transport becomes increasingly important in cases of essentially non-uniform forcing, located, for example, primarily in the tropics. These kinds of experiments were described by Alexeev et al. (2005) and showed that applying a tropical forcing of +4 W/m^2 to a 3D aquaplanet GCM without ice albedo feedbacks results in a more or less uniform global response. This could not be achieved if the atmospheric heat transport was not important since the extra-tropics did not have any external forcing in this experiment. The heat injected into the atmosphere by the warming tropical surface temperatures was uniformly distributed by the circulation of warmer and moister tropical air and forced the high latitudes to warm up. Clearly, this effect would have been observed with or without the presence of ice albedo feedback.

In some models polar amplification in 2 × CO_2 experiments may or may not be explained by properties of atmospheric heat transport. Albedo feedback in that case may seem to be working 'alone' and not requiring changes in atmospheric heat transport. However, even in this case the composition of that heat transport changes significantly, bringing more moisture in the air to the high latitudes while decreasing the sensible heat transport. This can result in significant changes in the radiative properties of the atmosphere, importantly, of non-local nature.

Acknowledgments VA was supported by Japan Agency for Marine Science and Technology (JAMSTEC) and NSF ARC 0909525. CJ would like to thank the International Arcitc Research Center and JAMSTEC for travel support while writing this article. Both authors would like to thank Igor Esau and the two anonymous reviewers for their valuable input that greatly helped improve the quality of the article.

References

Alexeev VA, Bates JR (1999) GCM experiments to test a proposed dynamical stabilizing mechanism in the climate system. Tellus 51A:630–651

Alexeev VA (2003) Sensitivity to CO_2 doubling of an atmospheric GCM coupled to an oceanic mixed layer: a linear analysis. Clim Dyn 20:775–787

Alexeev VA, Langen PL, Bates JR (2005) Polar amplification of surface warming on an aquaplanet in ghost forcing experiments without sea ice feedbacks. Clim Dyn 24:655–666

Arrhenius S (1896) On the influence of carbonic acid in the air upon the temperature of the ground. Philos Mag 41:237–276

Budyko M (1969) The effect of solar radiation variations on the climate of the Earth. Tellus 21(5):611–619

Cai M (2005) Dynamical amplification of polar warming. Geophys Res Lett 32:L22710

Cai M, Lu J (2007) Dynamical greenhouse-plus feedback and polar warming amplification. Part II: meridional and vertical asymmetries of the global warming. Clym Dyn 29:375–391

Flannery BP (1984) Energy-balance models incorporating transport of thermal and latent energy. J Atm Sci 41:414–421

Forest CE, Stone PH, Sokolov AP, Allen MR, and Webster MD (2002) Quantifying uncertainties in climate system properties with the use of recent climate observations. Science 295: 113–117

Graversen RG, Wang M (2009) Polar amplification in a coupled climate model with locked albedo. Clim Dyn 33:629–643

Hansen J, Sato M, Ruedy R, Nazarenko L, Lacis A, Schmidt GA, Russell G, Aleinov I, Bauer M, Bauer S, Bell N, Cairns B, Canuto V, Chandler M, Cheng Y, Del Genio A, Faluvegi G, Fleming E, Friend A, Hall T, Jackman C, Kelley M, Kiang N, Koch D, Lean J, Lerner J, Lo K, Menon S, Miller R, Minnis P, Novakov T, Oinas V, Perlwitz J, Perlwitz J, Rind D, Romanou A, Shindell D, Stone P, Sun S, Tausnev N, Thresher D, Wielicki B, Wong T, Yao M, Zhang S (2006) Efficacy of climate forcings. J Geophys Res 110:D18104

Holland MM, Bitz CM (2003) Polar amplification of climate change in coupled models. Clim Dyn 21:221–232

Hwang Y-T, Frierson DMW, Kay JE (2011) Coupling between arctic feedbacks and changes in poleward energy transport. Geophys Res Lett 38:L17704

IPCC (Intergovernmental Panel for Climate Change) (2007) Fourth assessment report. The physical sciences basis. Contribution of working group I to the fourth assessment report of the IPCC, Cambridge University Press, p 996

Kay JE, Holland MM, Bitz C, Blanchard-Wrigglesworth E, Gettelman A, Conley A, Bailey D (2012) The influence of local feedbacks and northward heat transport on the equilibrium Arctic climate response to increased greenhouse gas forcing in coupled climate models. J Clim 25:5433–5450

Langen PL, Alexeev VA (2004) Multiple equilibria and asymmetric climates in the CCM3 coupled to an oceanic mixed layer with thermodynamic sea ice. Geophys Res Lett 31:L04201. doi: 10.1029/2003GL019039

Langen PL, Alexeev VA (2005) A study of non-local effects on the Budyko-Sellers infrared parameterization using atmospheric general circulation models. Tellus 57A:654–661

Langen PL, Alexeev VA (2005) Estimating 2 × CO_2 warming in an aquaplanet GCM using fluctuation-dissipation theorem. Geophys Res Lett 32:L23708

Langen PL, Alexeev VA (2007) Polar amplification as a preferred response in an idealized aquaplanet GCM. Clim Dyn 29: 305–317

Lindberg K (2003) Supporting evidence for a positive water vapor/infrared radiative feedback on large scale SST perturbations from a recent parameterization of surface long wave irradiance. Meteorol Atmos Phys 84:285–292

Lu J, Cai M (2009) A new framework for isolating individual feedback processes in coupled general circulation climate models. Part I. Clim Dyn 32:873–885

Manabe S, Stouffer RJ (1988) Two stable equilibria of a coupled ocean-atmosphere model. J Clim 1:841–866

Murray FW (1967) On the computation of saturation vapor pressure. J Appl Meteorol 6:203–204

North GR (1975) Theory of energy-balance climate models. J Atmos Sci 32:2033–2043

Peixoto JP, Oort AH (1992) Physics of climate. Springer, New York, p 520

Rahmstorf S (1995) Bifurcations of the Atlantic thermohaline circulation in response to changes in the hydrological cycle. Nature 378:145–149

Robock A (1983) Ice and snow feedbacks and the latitudinal and seasonal distribution of climate sensitivity. J Atmos Sci 40: 986–997

Rodgers KB, Lohmann G, Lorenz S, Schneider R, Henderson GM (2003) A tropical mechanism for Northern Hemisphere deglaciation. Geochem Geophys Geosyst 4(5):10–46

Schneider EK, Lindzen RS, Kirtman BP (1997) A tropical influence on global climate. J Atmos Sci 54:1349–1358

Sellers WD (1969) A global climatic model based on the energy balance of the Earthatmosphere system. J Appl Meteorol 8: 392–400

Stone PH (1973) The effect of large-scale eddies on climatic change. J Atmos Sci 30(4):521–529